

Studying the Properties of Accretion Disks and Coronae in Black Hole X-ray Binaries with Monte-Carlo Simulation

Yangsens Yao^{1,2,3}, S. Nan Zhang^{1,2}, Xiaoling Zhang^{1,2}, Yuxin Feng^{1,2}, Craig R. Robinson⁴

ABSTRACT

Understanding the properties of the hot corona is important for studying the accretion disks in black hole X-ray binary systems. Using the Monte-Carlo technique to simulate the inverse Compton scattering between photons emitted from the cold disk and electrons in the hot corona, we have produced two table models in the *XSPEC* format for the spherical corona case and the disk-like (slab) corona case. All parameters in our table models are physical properties of the system and can be derived from data fitting directly. Applying the models to broad-band spectra of the black hole candidate XTE J2012+381 observed with BeppoSAX, we estimated the size of the corona and the inner radius of the disk. The size of the corona in this system is several tens of gravitational radius, and the substantial increase of the inner disk radius during the transit from hard-state to soft-state is not found.

Subject headings: accretion, accretion disks — black hole physics — X-rays: binaries — X-rays: individual (XTE J2012+381)

1. Introduction

A black hole X-ray binary (BHXB) system consists of a black hole (a compact object with mass $> 3M_{\odot}$) and its companion star. Material can be transferred from the companion to the black hole either through Roche lobe overflow or via a stellar wind (accretion process).

¹Physics Department, University of Alabama in Huntsville, Huntsville, AL 35899; yaoy@email.uah.edu, zhangsn@email.uah.edu, zhangx@email.uah.edu, fengyx@jet.uah.edu

²National Space Science and Technology Center, 320 Sparkman DR., SD50, Huntsville, AL 35805

³Present address: Department of Astronomy, University of Massachusetts, Amherst, MA 01003; yaoy@astro.umass.edu

⁴Division of Information Systems, National Science Foundation, 4201 Wilson Blvd, Arlington, VA 22230; crobinso@nsf.gov

Because the accreted matter must lose its angular momentum before it can be “swallowed” by the black hole, an accretion disk is usually formed and the gravitational potential energy of the accreted matter is released through radiation. The X-ray spectrum of a black hole X-ray binary system usually can be well fit with a two-component model: a black-body-like component and a power-law-like component (Tanaka & Lewin 1995). The black-body-like component turns off above 20 keV and is believed to be emitted from the accretion disk. The power-law-like component can extend up to several hundred keV, which suggests that a high temperature electron cloud (corona) exists above the accretion disk and the inverse Compton scattering between the disk photons and electrons in the corona is the main mechanism to produce this component.

In the X-ray astronomy community, the multi-color disk model (MCD) (*diskbb* in *XSPEC*, Mitsuda et al. 1984; Makishima et al. 1986) plus a power-law (PL) model has been employed traditionally to fit the energy spectra of BHXBs, then the parameters of the MCD model are used to infer the physical parameters of the accretion system. However, this model is over-simplified in the following two aspects.

First, the assumption that the power-law component extends straight to the low-energy limit of the spectrum is unreasonable, because the power-law component is believed to be produced by inverse Compton scattering. The most natural source of the seed photons is the thermal radiation from the accretion disk; they are of the same origin as the black-body-like component. Therefore a low-energy cutoff must be present in the power-law component, because the seed photon distribution has a peak energy, below which there are only a small amount of seed photons. Neglecting this low-energy cutoff by applying a simple power-law spectrum model would under-estimate the flux in the black-body-like component.

Second, it has been a rather standard approach by many (including some authors of this paper) in the field to take the black-body-like flux derived from the spectral model fitting as the true flux of the accretion disk and infer the inner disk radius from it. This ignores the radiative transfer process in the production of the power-law component. Since the power-law component is likely produced by scattering the soft photons in the original black-body-like component from the accretion disk, each photon in the power-law component comes at the expense of a lost photon in the black-body-like component, even if no absorption occurs in the Comptonization process. Therefore certain corrections are needed to infer the original flux of the black-body-like component, otherwise the real flux would be under-estimated, as realized by some authors (e.g., Kubota, Makishima & Ebisawa 2001), which might be the reason that the inner disk radius varies significantly when a BHXB transits from its hard state to its soft state or vice versa, like in XTE J1550-564 (Sobczak et al. 1999a), GRO J1655-40 (Sobczak et al. 1999b), XTE J2012+381 (Campana et al. 2002), etc..

In order to estimate the true flux of the accretion disk and then to estimate the inner disk radius, one needs to establish an intrinsic relation between the soft (low energy) photons and the hard (high energy) photons, then to make a radiative transfer correction to recover the original flux of the accretion disk, which makes it inevitable to calculate the Comptonized spectrum. The Comptonized spectrum has been computed by many authors using different approaches.

One of the analytical approaches was carried out by assuming an optically thick non-relativistic plasma and then solving the Kompaneets equation either numerically or analytically (e.g., Sunyaev & Titarchuk 1980; Payne 1980). This approach was improved later by Titarchuk (1994, T94 hereafter) and Titarchuk & Lyubarskij (1995) so that it could be applied to both non-relativistic and relativistic plasma, and was further verified by Hua & Titarchuk (1995, hereafter HT95) with different analytical approximations and Monte-Carlo simulations.

Another approach is to calculate radiative transfer with Monte-Carlo simulation (e.g., Corman 1970; Loh & Garmire 1971; Pozdnyakov, Sobol' & Sunyaev 1977; Fenimore et al. 1982; etc.). This method has been implemented and described in detail by Pozdnyakov, Sobol' & Sunyaev (1977, PSS77 hereafter), under the assumption that the probability for a collision between a photon and an electron is independent of the electron energy and the scattering angle. It was then significantly improved by Gorecki & Wilczewski (1984) by removing the above inaccurate assumption. The works mentioned above take the Compton scattering process as the main process when computing the Comptonized spectra from hot plasma, some other authors also take into account other important physical processes such as bremsstrahlung, pair production (e.g., Skibo et al. 1995) and disk-reflection (e.g., Haardt & Maraschi 1991).

Recently, Poutanen & Svensson (1996, hereafter PS96), by taking into account almost all important physical processes in the hot plasma and solving the radiative transfer equation iteratively for each scattering, built a new model to describe the emergent spectra from the plasma, which has been successfully tested with Monte-Carlo simulations (Stern et al. 1995).

The above works have been applied to both AGNs and X-ray binaries (e.g., Iwasawa et al. 2004; Wardzinski et al. 2002; Petrucci et al. 2000; Miller et al. 2004). In this paper, we only consider the Compton scattering process in the hot plasma (corona) and use the Monte-Carlo simulation to compute the emergent photon spectra. We stress on building a simple, self-consistent model in which the soft photons and the hard photons can be intrinsically linked and the radiative transfer process can be taken into account automatically. Therefore, the physical parameters of the corona, as well as the parameters of the accretion disk, can be directly derived from the spectral fitting with the model. We will discuss the difference

between our model and the power-law model, especially in deriving the inner disk radius when applied to BHXBs.

This paper is organized as following. In section 2, our Monte-Carlo simulation is introduced, in section 3 the results of applying our table models to the source XTE J2012+381 is reported, and summary and discussion are presented in section 4.

2. Monte-Carlo Simulations and Table Models

2.1. Assumptions and Simulations

In our simulations, we assume that the accretion disk is an optically thick Keplerian disk (Mitsuda et al. 1984), and during the accretion process, the accretion rate (\dot{m}) is constant and the gravitational potential energy loss of the accreted material is radiated away in blackbody radiation locally. Therefore the temperature radial profile is $T(r) \sim r^{-3/4}$, as in the MCD model (Mitsuda et al. 1984; Makishima et al. 1986). We also assume that the corona above the accretion disk may take either spherical or disk geometry, the electron density distribution in the corona is uniform, and the electron energy distribution in the corona follows a thermal form as assumed in previous works (HT95, T94, PS96); the disk reflection is ignored, and the corona is in stationary equilibrium.

We sample photons for a given combination of the parameters, i.e., the temperature at the inner boundary of the accretion disk, the size of the corona (for a spherical corona system, the size is defined as the value of its radius; for a disk-like corona system, it is defined as the vertical height), the temperature of the electrons in the corona, and the optical depth of the corona (defined as $\tau = \int n_e \sigma_T dl$, where n_e is electron density, σ_T is Thompson scattering cross section and the integral is along the radial direction in the spherical corona case or along the vertical direction in disk-like corona case). Since the radiation is taken as a black body locally, the number of photons released from a ring on the accretion disk is,

$$\begin{aligned} dN_{ph} &= a^* T^3 2\pi r dr \\ &\propto r^{-5/4} dr, \end{aligned} \tag{1}$$

where

$$a^* = \frac{2\pi}{c^2} \left(\frac{k}{h}\right)^3 \int_0^\infty \frac{x^2 dx}{e^x - 1},$$

c is the speed of light, k is Boltzmann's constant and h is Planck's constant. The photon energies follow blackbody distribution with temperature $T(r)$ and the initial direction of a photon is sampled uniformly in 4π solid angles. In a spherical corona system, the corona

covers a portion of the disk, then a photon emitted from the disk may or may not enter the corona, depending upon the emitting location and the initial direction. In disk-like corona systems the corona covers the whole disk, so a photon emitted from the disk always enters the corona first.

After a photon enters the hot corona, the probability (ρ) for it to interact with an electron is determined by its free-path distance,

$$d\rho \propto e^{-\tau_l} d\tau_l, \quad (2)$$

and

$$d\tau_l = \sigma_{K-N} n_e dl, \quad (3)$$

where τ_l is the optical depth of the free-path distance along the moving direction, σ_{K-N} is Klein-Nishina cross section (Berestetski et al. 1972),

$$\sigma_{K-N}(x) = 2\pi r_0^2 \frac{1}{x} \left[\left(1 - \frac{4}{x} - \frac{8}{x} \right) \ln(1+x) + \frac{1}{2} + \frac{8}{x} - \frac{1}{2(1+x)^2} \right], \quad (4)$$

and

$$x = \frac{2h\nu}{m_e c^2} \gamma (1 - \bar{v} \cdot \bar{\Omega}/c),$$

$h\nu$, $\bar{\Omega}$ are the energy and the direction of the incident photon, respectively, and \bar{v} is the electron velocity, all in the laboratory frame; r_0 is the classical electron radius ($r_0 = e^2/mc^2$) and $m_e c^2$ is the electron rest energy. It is obvious that σ_{K-N} depends on the incident photon energy, electron energy and their moving directions. In order to determine the photon free-path distance l in equation 3, we need to calculate σ_{K-N} , therefore we need to know the electron energy (E_e) along a sampled direction, which usually is a function of the photon's free-path distance, i.e., the dependency relation for equation 3 is like, $l \rightarrow \sigma_{K-N} \rightarrow E_e \rightarrow l$. To simplify this problem, we assume that the energy distribution in the corona is uniform, then the dependency between E_e and l is no longer needed. However, the sampling of the electron velocity is not trivial, because it is related to the input photon information and the total Compton cross section $\sigma_{K-N}(x)$,

$$\rho(\bar{v}) \propto N(\bar{v}) (1 - \bar{v} \cdot \bar{\Omega}/c) \sigma_{K-N}(x), \quad (5)$$

where, $N(\bar{v})$ is electron distribution which is further assumed to be isotropic and follows a thermal form $dN_e \propto e^{-E_e/kT} \sqrt{E_e} dE_e$, T is the temperature of the corona.

Equation 5 is a two-dimensional probability distribution, which is rather complicated to obtain and has been addressed in previous works (Sobol' 1974; Gorécki & Wilczewski 1984). In our simulation, we adopt the algorithm developed by Hua (1997) to sample the

electron energy E_e and its moving direction $\bar{\Omega}_e$. Therefore σ_{K-N} can be calculated (the photon energy and moving direction are known) and the photon's free-path distance can be derived using equation 3.

After each interaction, the scattered photon direction can be sampled by using the differential cross section (Akhiezer & Berestetski 1965), which is a function of electron velocity (\bar{v}), the incident photon energy and direction, and the scattered photon energy. In the electron's rest frame, the formula is relatively simple (Klein & Nishina 1929),

$$\frac{d\sigma}{d\Omega} = \frac{1}{2}r_0^2 \left(\frac{h\nu}{h\nu_i} \right) \left(\frac{h\nu}{h\nu_i} + \frac{h\nu_i}{h\nu} - \sin^2 \theta \right), \quad (6)$$

where θ is the scattering angle, $h\nu_i$ and $h\nu$ are respectively the incident photon energy and the scattered photon energy in the electron's rest frame and related to each other by

$$h\nu = \frac{h\nu_i}{1 + \frac{h\nu_i}{m_e c^2} (1 - \cos \theta)}. \quad (7)$$

Therefore, after sampling the electron energy and direction, we transform the incident photon information to the electron's rest frame, and substitute the scattered photon energy ($h\nu$) in equation 6 with equation 7, then the scattered photon direction can be sampled. In the end, the scattered photon energy can be calculated easily.

After zero or more scattering with electrons, an incident photon will escape and the escaped photons will form a spectrum, which depends on the inclination angle. In our simulation, we ignore the disk reflection, i.e., a photon is assumed to be absorbed by the accretion disk when it collides with the disk.

It is worth noting that unlike the method described by Gorecki & Wilczewski (1984), we trace each single photon from its emitted location until it escapes from the disk-corona system, then record it as a single event, i.e., each recorded photon has exactly the same statistical weight as others. In this manner, we sacrifice the simulation efficiency to avoid calculating the escape probability and the scattering probability distribution in each scattering. Therefore our Monte-Carlo code has been sufficiently simplified and its efficiency obviously depends on the configuration of the disk-corona system (especially on the optical depth of the corona); the total computation time is also tolerable (e.g., it takes 5 minutes to produce 500,000 events for a spherical corona with optical depth around unity when running on a 1.50 GHz Intel Xeon CPU).

2.2. Simulation Summary and Comparison with the Previous Works

For a spherical corona system, Figure 1 summarizes the dependency of simulated spectra on the input corona parameters (corona temperature T_c , opacity τ , and size R_c) as well as on the input disk properties (inner disk temperature T_{in} and disk inclination angle θ). For a disk-like corona, the emergent spectra have the similar dependency except for R_c and θ , because in this case, R_c is defined as the vertical height of the corona and the corona always covers the accretion disk, therefore R_c is solely determined by τ under the uniform density assumption. For the dependency on θ , in a spherical corona system, the flux of the soft component of the spectrum at different inclination angle differs by a cosine factor due to the projection effect, whereas the hard component is nearly isotropic except for at very high θ (Figure 2.a) because τ does not depend on θ . Strictly speaking, the effective optical depth is slightly different for different θ if we consider the seed photon distribution along the accretion disk and this difference is obvious when the inclination angle of the disk is high. However, in a disk-like corona system, in addition to the effective area due to the projection, the effective optical depth of the corona also depends on the viewing angles, therefore both the soft flux and the hard flux are related to θ by a cosine-like factor (Figure 2.b).

We compare the angle-averaged Comptonized spectra calculated from our simulation with those from the analytic formulae for thermal Comptonization by T94, and with those obtained from the iterative scattering method by PS96 (Figure 3). In our simulation and the calculation by PS96, the incident photons are from the center of a spherical corona and follow the Planck’s formula, whereas in the computation by T94, the incident photons were assumed to follow the Wien form. The key parameters of the corona, T_c and τ , are also listed in Figure 3. The comparison implies that, for our work and the works of T94 and PS96, the results are fairly consistent with each other when the corona is optically thin ($\tau_c \leq 1$); when the corona is optically thick ($\tau_c \geq 2$) the differences between all the works become visible.

2.3. Table models

Based on the simulated spectra, we have built two *XSPEC* format table models¹, one for spherical corona system and one for disk-like corona system. The table models consist of the following parameters: temperature at the inner boundary of the accretion disk (T_{in}), thermal electron temperature in the corona (T_c), radial size of the spherical corona (R_c , in unit of $R_g = GM/c^2$, where M is the black hole mass), optical depth of

¹ftp://legacy.gsfc.nasa.gov/caldb/docs/memos/ogip_92_009/ogip_92_009.ps

the corona (τ), inclination angle of the accretion disk (θ), and normalization parameter (K_{norm}) which is added by the *XSPEC* automatically and related to the disk radius by $K_{norm} = ((R_{in}/km)/(D/10kpc))^2$, where D is the distance of the source (see Appendix for detail). Because for the disk-like corona R_c is redundant, it does not appear in the table models for the disk-like corona. In §3, we will apply these two models to BHXB XTE J2012+381.

3. Application to XTE J2012+381

The X-ray transient XTE J2012+381 was discovered with the All Sky Monitor aboard Rossi X-ray Timing Explorer on May 24, 1998 (Remillard et al. 1998). Its spectra observed with ASCA consist of a soft thermal component (with temperature around 0.8 keV) and a hard power-law tail (with photon index around 3) (White et al. 1998), which is considered to be indicative of a black hole candidate (Lewin, Van Paradijs & Van Den Heuvel 1995). Five observations were carried out with BeppoSAX from 1998 May 28 to 1998 July 8 (Fig 4.a). The spectra with the narrow field instruments LECS (Parmar et al. 1997) and MECS (Boella et al. 1997) were extracted within a circular region with a radius of 8' centered at the source position. The background for these two instruments were obtained using blank sky observations. HPGSPC (Manzo et al. 1997) and PDS (Frontera et al. 1997) data were extracted using SAXDAS (hproducts V3.0.0) and XAS respectively. All our spectral analysis were carried out in the energy range suggested by the BeppoSAX cookbook²: 0.12-4 keV for the LECS, 1.65-10.5 keV for MECS, 8-20 keV for the HPGSPC, 15-220 keV for PDS, and a 2% systematic error were added during the fitting to account for the uncertainties in the calibration. The public software package *XSPEC* 11.0.1 was employed in our analysis.

As usual, MCD plus a power-law and a Gaussian line model was used first to fit the data, which can describe the observations very well (refer to Figure 4(b)). The best fit parameters are similar to the previous results reported by Campana et al. (2002).

Our two table models plus a broad Gaussian line were then applied to the data, and these two models provide reasonably good fit to all the BeppoSAX observations (Figure 4(c)-4(d)) and the best fit parameters are reported in Table 1. Since we mainly focus our efforts on the continuum, the line parameters are not listed.

According to the fitting results, the column density nearly remains constant with a mean central value $1.33 \times 10^{22} \text{ cm}^{-2}$, and T_{in} is around 0.72 keV, which agree with the previous

²<http://heasarc.gsfc.nasa.gov/docs/sax/abc/saxabc/saxabc.html>

report (Campana et al. 2002). T_c decreases during the BeppoSAX observations. In the first two observations, the upper limit of T_c is even beyond the parameter range (current range is 5 keV to 200 keV) in our table models. In the last three observations, the spectra are relatively soft and T_c can be constrained tightly. If the system has a spherical corona, R_c may vary from several tens to one hundred times of the gravitational radii. The optical depth τ is very small (< 0.5) for all the five observations, and the θ values are with a large uncertainty. The normalization parameter, K_{norm} , which is related to the inner disk radius, also varies dramatically in the five observations. However, this apparent variation is caused by the uncertainty of θ (see discussion below). In order to further check the variation, we re-normalize K_{norm} to the value at zero inclination angle, and plot the inner disk radius ($R_{in} = \sqrt{K_{norm} \cos \theta}$ km) for different observations (Figure 5). For comparison, we also plot the results from the MCD+PL model (Campana et al. 2002) in the figure. Even though with large uncertainties, R_{in} derived from our models are consistent with being constant, within the error bars (90%) and the “sharp” increase of R_{in} derived from MCD+PL model does not show up in our results.

4. Discussion

In this work, we developed a Monte-Carlo code to simulate the scattering process between the seed photons from an accretion disk and the electrons in the corona above the disk. Based on the simulation results, we build two simple table models for the spherical corona system and for the disk-like corona system, which can be used in the spectral fitting to directly derive the corona properties (like its size, opacity, and temperature) as well as the disk parameters (disk temperature, inclination and inner disk radius).

The reason that the size of the spherical corona can be determined from the X-ray spectral fitting is that in our models the seed photons for the inverse Compton scattering come from the disk, on which the temperature is a function of the distance from the central black hole. The relatively small size of the corona of XTE J2012+381 obtained in this work indicates that the hard photons are mainly generated within a very small region near the central black hole.

The opacity of the corona can be inferred from the ratio between the flux of the soft component and that of the hard component, whereas the temperature of the corona can be determined by the high energy turn over in the spectrum. However, for XTE J2012+381, the τ we obtained is rather small, indicating only a small portion of the disk photons were up-scattered to the high energies. When the source was in its hard spectral state (e.g., the first observation), we did not see an obvious turn-over in the spectrum, which may suggest that

the pure thermal corona is not a good approximation in this case and should be replaced by the thermal-powerlaw hybrid corona, a more realistic one proposed by Coppi (1999). When the source was in its soft spectral state (the last two observations), we obtained a low corona temperature T_c , which suggests that a large uncertainty may exist in the inferred corona parameters, because the disk emission could be mixed with the corona emission and any slight change of the disk parameter (e.g., inclination angle) could result in apparently significant change of the corona parameters. Even though these changes will also cause some changes in the K_{norm} parameters of our table model, our conclusion marks are based on the re-normalized K_{norm} (to zero degree for example) which can be hardly impacted.

The reason that the inclination angle can in principle be inferred is that the observed flux from the disk depends strongly upon the inclination angle (through a cosine factor), whereas the hard X-ray flux resulting from Compton scattering is almost isotropic for the case of spherical corona. For the case of disk-like corona, the hard X-ray flux also depends upon the disk inclination angle. However, the inclination angle, which is also related to the ratio between the soft component flux and the hard component flux, is always coupled with the optical depth of the corona. Thus, inferring the disk inclination angle by spectral fitting may have some ambiguities.

Determining the value of the inner disk radius is important for understanding the physics of the accretion disk and the black hole angular momentum (Zhang et al. 1997). The normalization parameter inferred with our table model, which is proportional to the inner disk radius squared, is nearly constant in the BeppoSAX observations, and the previously reported sharp increase of the disk radius when the source transits from the hard state to the soft state did not happen. This is because the corona, though optically thin in most cases, scatters some of the photons emitted from the disk and makes the observed soft component different significantly from the original disk emission. Using the simple MCD+PL model and without considering the origin of the PL like component will certainly under-estimate the real flux of the blackbody-like component, especially when the source is in the hard state. The reason that we can estimate the real flux of the accretion disk is that the number of the photons emitted from the disk is known in our Monte-Carlo simulations.

In our simulation process, we did not include the reflection mechanism to produce a reflection component in the emergent spectrum, but simply ignored a sampled photon when it collides with the accretion disk. Even though the ignored photons will not be reflected in the output spectrum, their corresponding seed photons are still counted as part of the original disk emission. A disk reflected spectrum is potentially important for probing the disk ionization parameter, the geometry, the inclination angle of the accreting system. When the disk reflected component is clearly visible in a spectrum (e.g., in Cyg X-1; Salvo et al. 2001),

the Comptonization model developed in this work plus a reflection model can be utilized to account for the observed total spectrum. As long as the combined model can fit the observed spectrum satisfactorily, the original disk flux could still be reconstructed from the normalization of the table model.

Please also be noted that in this work we did not consider the vertical structure of the accretion disk (e.g., Shimura & Takahara 1995) and the gravitational potential is still assumed to be the Newtonian potential, therefore, the derived inner disk radius in this work might be substantially different from the “real” value. In fact, because of the high temperature ($\sim 1keV$) around the inner disk region, the Compton scattering process may dominate over the free-free process in this region, and the local emergent spectrum might be approximated as a diluted blackbody spectrum rather than a real black body spectrum. The spectral difference due to this effect can be corrected by the spectral hardening factor, which is ~ 1.7 for an accreting system at about 10% accretion rate (Shimura & Takahara 1995). The correction for the real potential in the vicinity of the black hole (general relativity effects) could be done by introducing three factors η , f_{GR} , g_{GR} . The η accounts for the difference between the apparent and the intrinsic radii of the peak temperature, and the f_{GR} is due to temperature change caused by the gravitational red shift and Doppler shift, whereas the g_{GR} is related to the integrated flux change caused by the gravitational focusing and boosting. The value of these factors, depending on the system inclination and black hole spin, have been discussed in several papers (Shakura & Suniaev 1973; Cunningham 1975; Ebisawa et al. 1994) and also have been tabulated by Zhang et al. (1997), which have been proved to be reasonably accurate (Gierliński et al. 1999, 2001). We should point out that all these corrections, if performed in this study, will systematically change the values of the derived inner disk radii but will hardly change the conclusion that the inner disk radius is nearly constant (this situation has been proved when applying the same model and the above corrections to the six ultra-luminous X-ray sources (Wang et al. 2004)).

In our table model, the normalization parameter is very sensitive to the inclination angle, which, as mentioned before, is coupled together with the optical depth. In order to reduce the uncertainty of the value of the normalization parameter in our table model and to infer the real flux of the accretion disk, an accurate value of the inclination angle is needed and the optical observations may give useful help on this issue.

We thank the anonymous referee for critical, yet insightful comments on our manuscript, which made us to improve the paper substantially. Mr. Yongzhong Chen is acknowledged for his initial work on this project during his visit to UAH in 1999-2000. We want to give our special thanks to Dr. S. Campana for kindly giving us the data of XTE J2012+381 observed with BeppoSAX. We also thank Drs. Lev Titarchuk and Wei Cui for interesting

discussions and Dr. Alan Harmon for useful comments. This work was supported in part by NASA Marshall Space Flight Center under contract NCC8-200 and by NASA Long Term Space Astrophysics Program under grants NAG5-7927 and NAG5-8523.

A. Normalization parameter in our table models

Starting from a multi-color disk black body, assuming the inner disk temperature is T_{in} and the inner disk radius is R_{in} , then the total number of photons released by the disk per unit time will be (by integrating Plank function from R_{in} to infinity),

$$ph = 8\pi a^* T_{in}^3 r_{in}^2 \quad (\text{A1})$$

where, $a^* = \frac{2\pi}{c^2} \left(\frac{K}{h}\right)^3 \int_0^\infty \frac{x^2 dx}{e^x - 1}$. Thus, the observed photon flux at distance D with inclination angle θ will be,

$$\begin{aligned} F_{ph}(\theta) ds &= ph(\theta) d\Omega \\ &= 8 \cos(\theta) a^* T_{in}^3 r_{in}^2 \frac{ds}{D^2} \\ &= 8 \cos(\theta) a^* T_{in}^3 \left(\frac{r_{in}}{D}\right)^2 ds. \end{aligned} \quad (\text{A2})$$

If considering the double sides of the accretion disk, there should be another factor 2 in equation (A1) and (A2). However, in our calculation, we only consider one side and it is self-consistent within our table model.

In our simulation, for each configuration of the parameters, 500,000 photons are collected. Because the black hole (BH) absorption and the collision between the photons and the accretion disk (we ignore the disk reflection), the seed photon number $N_{seed} \geq 500,000$. In each simulation, six spectra will be produced by collecting the output photons in different directions from 0° to 35° , 35° to 45° , 45° to 55° , 55° to 65° , 65° to 75° , 75° to 85° degrees, corresponding to the inclination angles 22.7, 40.1, 49.9, 59.8, 69.6, 79.2 degrees respectively (by considering the solid angle and disk projection). To make a connection between the seed photon number in our simulation and the real disk flux, each spectrum had been scaled down by a factor f_{scale} , which is determined by,

$$f_{scale} = N_{seed}/ph \quad (\text{A3})$$

To get the spectrum observed at different inclination angles, each angle-dependent spectrum has been scaled down by different area factors Δs_θ to get the average flux at that inclination angle, which is determined by,

$$\begin{aligned} \Delta s_\theta &= \int_{\theta_i}^{\theta_j} D^2 \sin(\theta) d\theta \int_0^{2\pi} d\phi \\ &= 2\pi D^2 [\cos(\theta_i) - \cos(\theta_j)] \end{aligned} \quad (\text{A4})$$

If we take $r_{in} = 1$ km, $D = 10$ kpc in equation (A2) (in order to compare with *diskbb* in *XSPEC*), the relation between real r_{in} and normalization of the table model is,

$$K_{norm} = \left(\frac{r_{in}/km}{D/10kpc} \right)^2 \quad (\text{A5})$$

REFERENCES

- Akhiezer, A. J. & Berestetski, V. B. 1965, Quantum Electrodynamics (New York: Interscience Publications).
- Berestetski, V. B., Lifshitz, E. M., & Pitaevski, L. P. 1972, Relativistic Quantum Theory (Oxford, New York: Pergamon Press).
- Boella, G., Chiappetti, L., Conti, G., Cusumano, G., del Sordo, S., La Rosa, G., Maccarone, M. C., Mineo, T., Molendi, S., Re, S., Sacco, B. & Tripiciano, M. 1997, A&AS, 122, 327
- Campana, S., Stella, L., Belloni, T., Israel, G. L., Santangelo, A., Frontera, F., Orlandini, M. & Dal Fiume, D. 2002, A&A 384, 163
- Coppi, P. S. 1999, Invited review at the workshop “High Energy Process in Accreting Black Holes”, eds. J. Poutanen and R. Svensson, ASP Conf. Series, Vol. 161, P.375 (astro-ph/9903158)
- Corman, E. G. 1970, Phys. Rev., D1, 2734
- Cunningham, C. T. 1975, ApJ, 202, 788
- Ebisawa, K. et al. 1994, PASJ, 46, 375
- Fenimore, E. E., Klebesadel, R. W., Laros, J. G., Stockdale, R. E. & Kane, S. R. 1982, Nature, 297, 665
- Frontera, F., Costa, E., dal Fiume, D., Feroci, M., Nicastro, L., Orlandini, M., Palazzi, E. & Zavattini, G. 1997, A&AS, 122, 357
- Gierliński, M., Zdziarski A. A., Poutanen J., Coppi P. S., Ebisawa K., & Johnson W. N., 1999, MNRAS, 309, 496
- Gierliński, M., Maciołek-Niedźwiecki, A., and Ebisawa, K. 2001, MNRAS, 325, 1253
- Gorécki, A. & Wilczewski, W. 1984, Acta Astron., 34, 141

- Haardt F. & Maraschi, L. 1991, ApJ380, L51
- Hua, X.-M. & Titarchuk, L. 1995, ApJ, 449, 188
- Hua, X.-M. 1997, Computers in Physics, Vol. 11, No. 6
- Iwasawa, K., Lee, J. C., Young, A. J., Reynolds, C. S., Fabian, A. C. 2004, MNRAS, 347, 411
- Klein, O. & Nishina, Y. 1929, *Zs. f. Phys*, 52, 853
- Kubota, A., Makishima, K. & Ebisawa, K. 2001, ApJ, 560, L147
- Lewin, W. H., Van Paradijs, J. & van den Heuvel, E. P. J. 1995, X-Ray Binaries, Cambridge University Press, ISBN 0-521-59934-2
- Loh, E. D. & Garmire, G. P. 1971, ApJ166, 301
- Makishima, K., Maejima, Y., Mitsuda, K., Bradt, H. V., Remillard, R. A., Tuohy, I. R., Hoshi, R. & Nakagawa, M. 1986, ApJ 308, 635
- Manzo, G., Giarrusso, S., Santangelo, A., Ciralli, F., Fazio, G., Piraino, S. & Segreto, A. 1997, A&AS, 122, 341
- Miller, J. et al. 2004, ApJ, 606, L131
- Mitsuda, K., Inoue, H., Koyama, K., Makishima, K., Matsuoka, M., Ogawara, Y., Suzuki, K., Tanaka, Y., Shibazaki, N. & Hirano, T. 1984, PASJ, 36, 741
- Parmar, A. N., Martin, D. D. E., Bavdaz, M., Favata, F., Kuulkers, E., Vacanti, G., Lamers, U., Peacock, A. & Taylor, B. G. 1997, A&AS, 122, 309
- Payne, D. G. 1980, ApJ, 237, 951
- Petrucci, P. O. et al. 2000, ApJ, 540, 131
- Poutanen, J. & Svensson, R. 1996, ApJ, 470, 249
- Pozdnyakov, L. A., Sobol, J. M. & Sunyaev, R. A. 1977, Sov. Astron.-AJ, 21 708
- Remillard, R., Levine, A., Wood, A., Wagner, R. M., Starrfield, S., Shrader, C., Bowell, E., Skiff, B. & Koehn, B. 1998, IAUC 6920
- Salvo, T. D. et al. 2001, ApJ, 547, 1024

- Shakura, N. I. & Suniaev, R. A. 1973, *A&A*, 24, 337
- Shimura, T & Takahara, F. 1995, *ApJ*, 445, 780
- Skibo, J., G., Dermer, C. D., Ramaty, R. & McKinley, J. M. 1995, *ApJ*, 446, 86
- Sobczak, G. J., McClintock, J. E., Remillard, R. A., Levine, Alan M., Morgan, E. H., Bailyn, C. D. & Orosz, J. A. 1999a, *ApJ*, 517, L121
- Sobczak, G. J., McClintock, J.E., Remillard, R. A., Bailyn, C. D. & Orosz, J. A. 1999b, *ApJ*, 520, 776
- Sobol', J. M. 1974, *The Monte-Carlo Methods* (The University of Chicago Press).
- Stern, B. E., Poutanen, J., Svensson, R., Sikora, M. & Begelman, M. C. 1995, *ApJ*, 449, L13
- Suniaev, R. A. & Titarchuk, L. G. 1980, *A&A*, 86, 121
- Tanaka, Y. & Lewin, W. 1995, in *X-ray Binaries*, eds. W.H.G. Lewin, J. van Paradijs, & E.P.J. van den Heuvel, Cambridge U. Press, Cambridge) 126
- Titarchuk, L. 1994, *ApJ*, 434, 570
- Titarchuk, L. & Lyubarskij, Y 1995, *ApJ*, 450, 876
- Wang, D., Yao, Y., Fukui W., Zhang, S. N., & Williams, R. 2004, *ApJ*, 609, 113
- Wardzinski, G. et al. 2002, *MNRAS*, 337, 829
- White, N. E., Ueda, Y., Dotani, T. & Nagase, F. 1998, *IAUC* 6927
- Zhang, S. N., Cui, W & Chen, W. 1997, *ApJ*, 482L, 155Z

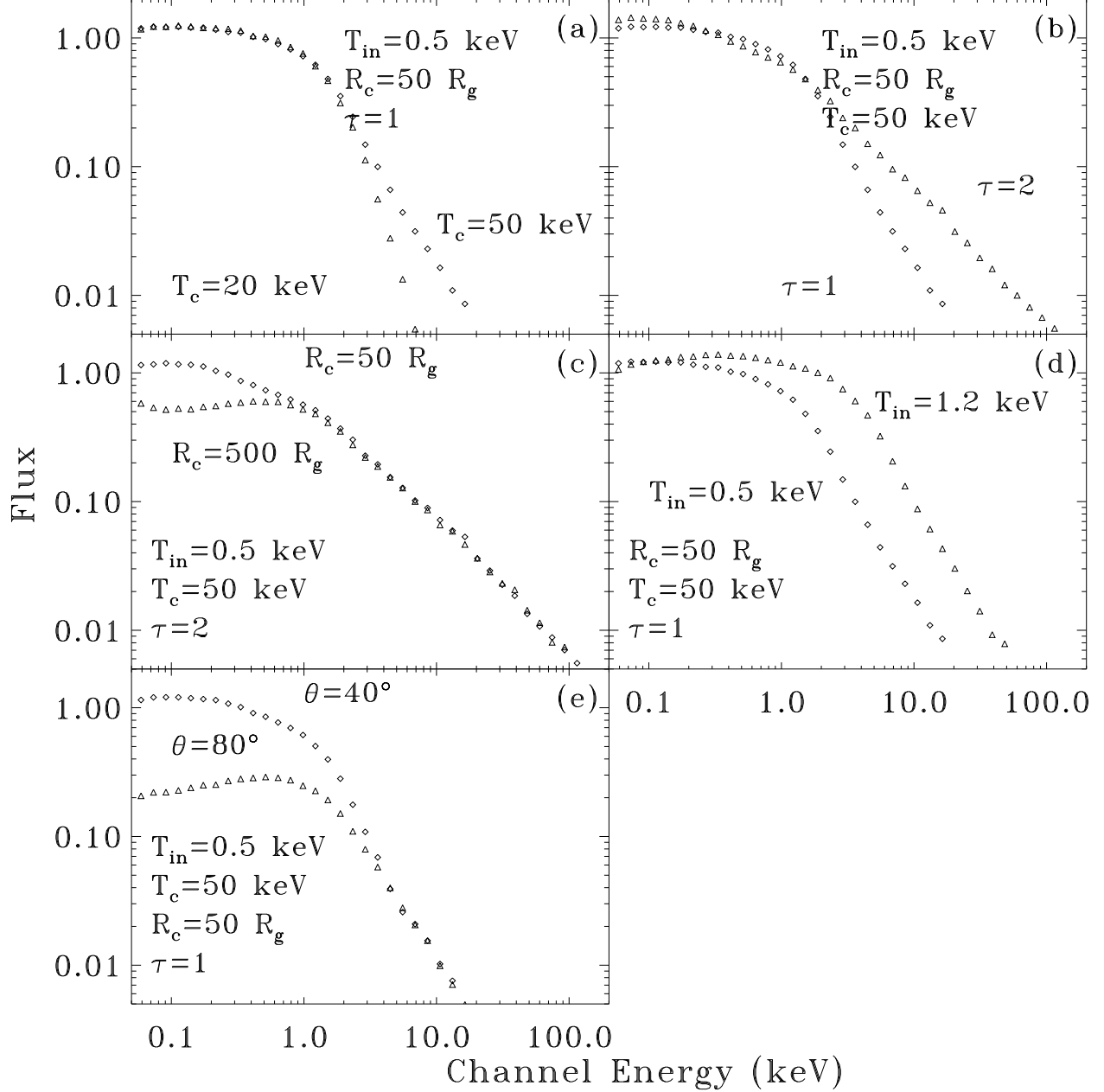


Fig. 1.— The angle-averaged simulated spectrum as a function of (a) corona temperature, (b) corona opacity, (c) corona size, (d) inner disk temperature, and emergent spectra as a function of the disk inclination angle (e).

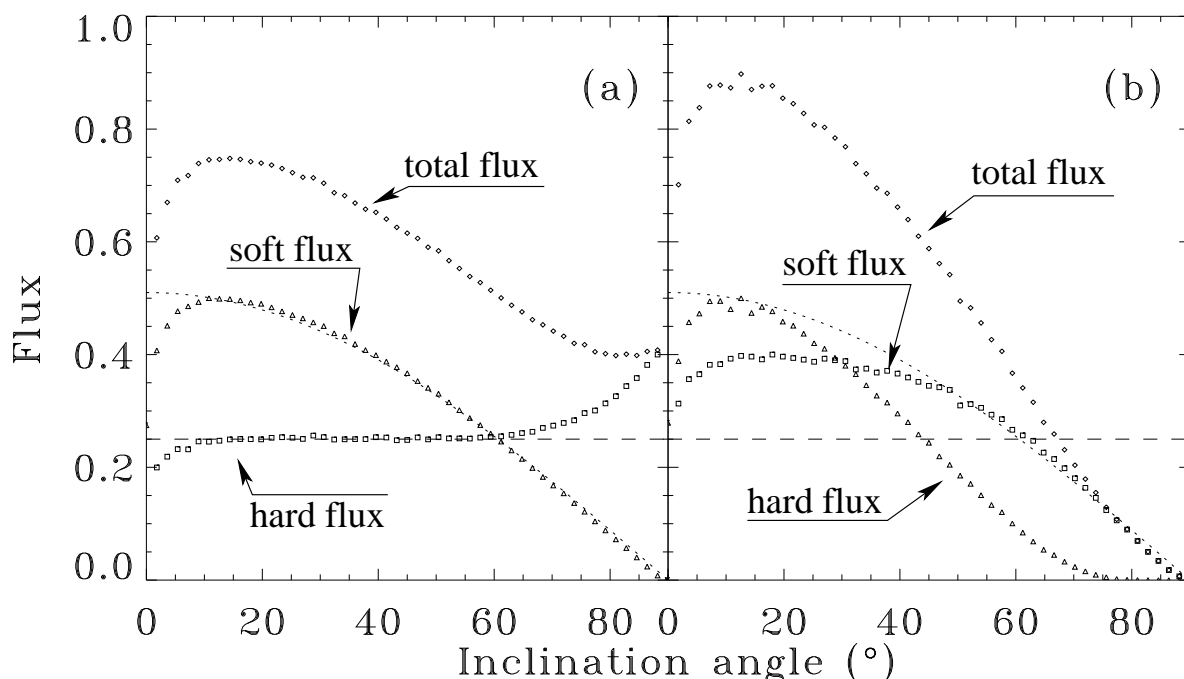


Fig. 2.— The flux dependency on the inclination angle in a spherical corona system (a) and in a disk-like corona system (b). The *dotted line* indicates a scaled cosine function and the *dashed line* indicates a constant value. The *hard flux* indicates the photons with at least one scattering and the *soft flux* indicates the photons without any scattering. The turn-off in the low angle end is artificial (the counting statistic is poor).

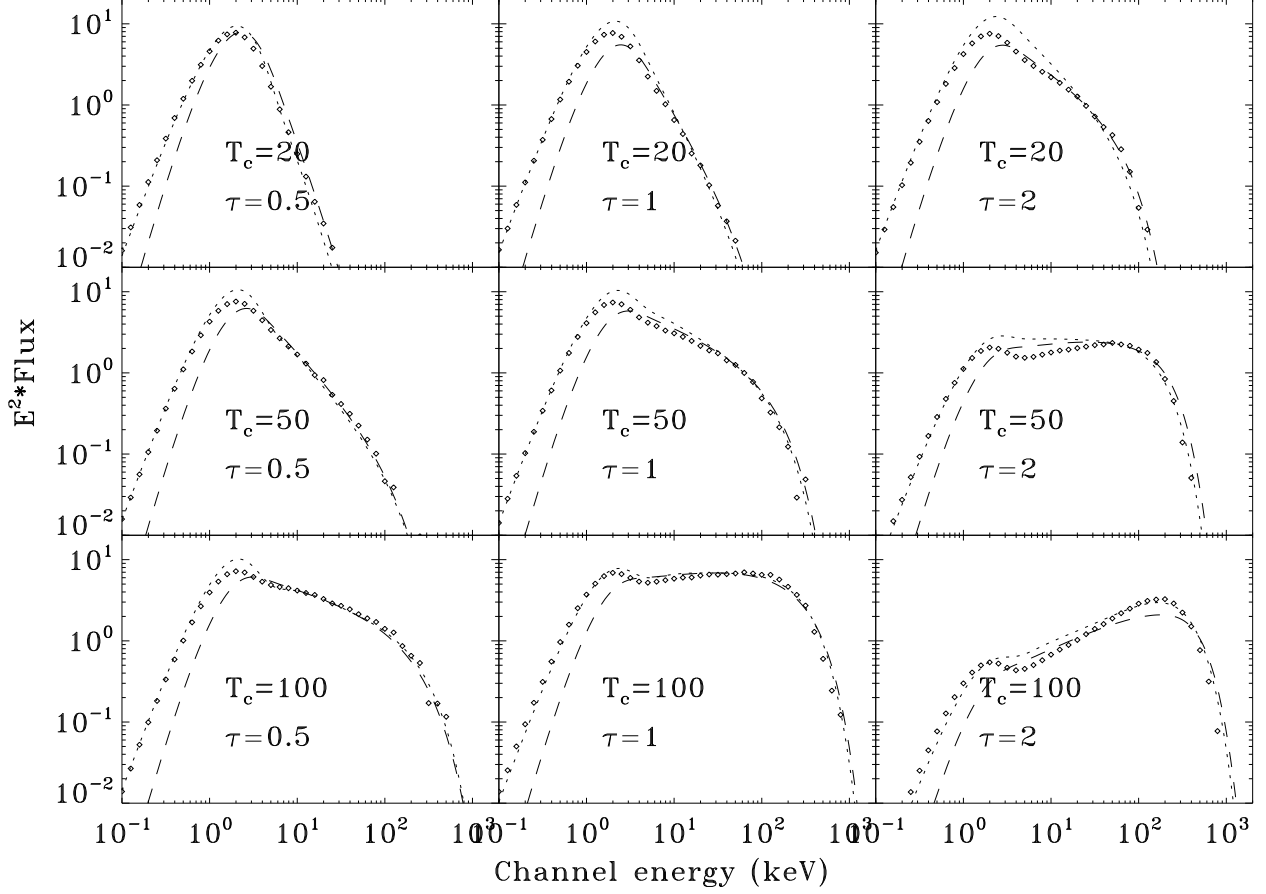


Fig. 3.— Angle-averaged Comptonized spectra $E^2*\text{Flux}$ from a spherical corona. The incident photons are assumed from the center of the corona. The *diamond symbols*: results from our simulation; *dotted line*: results from Poutanen & Svensson (1996); *dashed line*: results from Titarchuk (1994). T_c is the electron thermal temperature in the corona and τ is the Thomson optical depth of the corona. See text for detail.

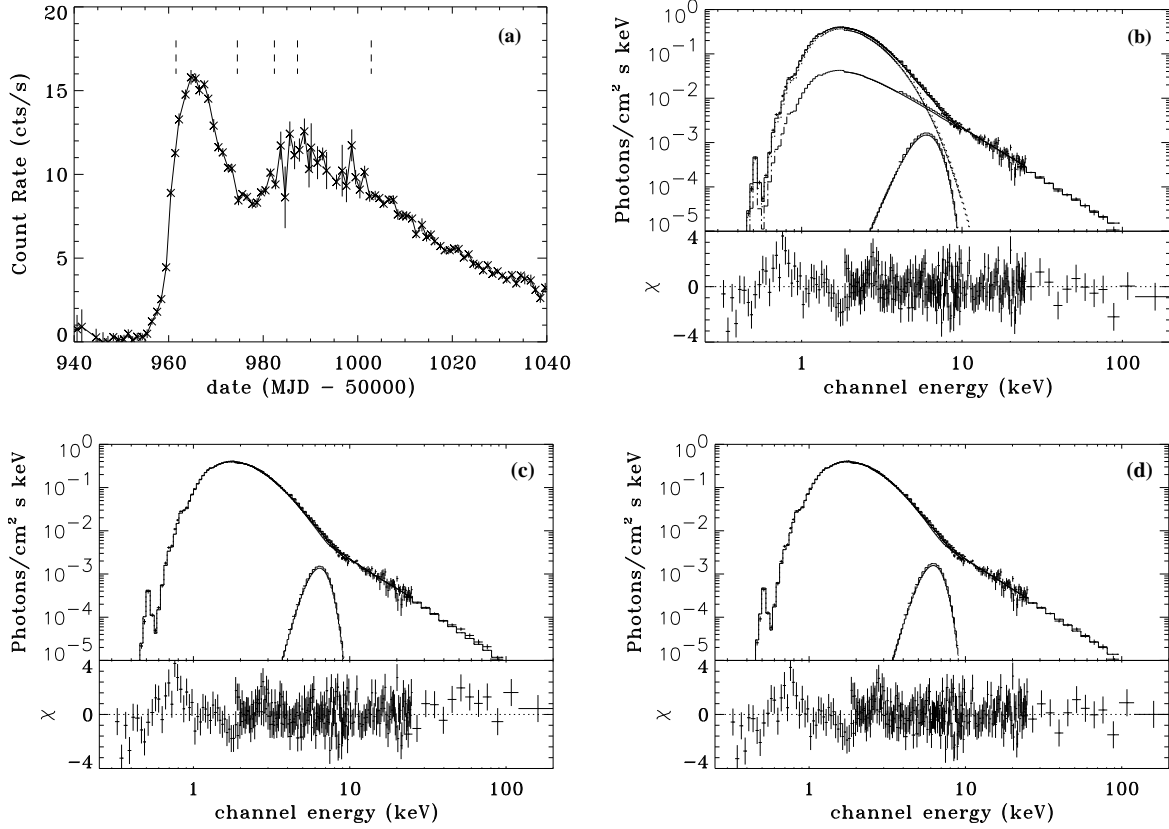


Fig. 4.— Panel (a) is the ASM/RXTE light curve of the black hole candidate XTE J2012+381 during its outburst in 1998; the dotted lines indicate the dates of BeppoSAX observations we have analyzed. The first observation is in the rising phase in which the hard component is relatively strong whereas the other four observations are in the soft state. Panel (b) shows the unfolded spectrum and the residuals for the first observation modeling with MCD+PL with inter-stellar absorption and a Gaussian line. The best fit parameters are: $N_H = 1.36 \pm 0.02 \times 10^{22} \text{ cm}^{-2}$, $T_{in} = 0.75 \pm 0.01 \text{ keV}$, $K_{BB} = 1097 \pm 50$, $\Gamma = 2.22 \pm 0.04$, $norm = 0.32 \pm 0.05$, $E_{gauss} = 6.1 \pm 0.2 \text{ keV}$, $\sigma_{gauss} = 1.0 \pm 0.2 \text{ keV}$, $norm_{gauss} = (3.5 \pm 0.4) \times 10^{-3}$, and χ^2 is 277 with 244 degrees of freedom. Panels (c) and (d) are unfolded spectra and the residuals for the first observation modeling with our table models for a spherical corona system and for a disk-like corona system respectively. The best fit parameters are presented in Table 1.

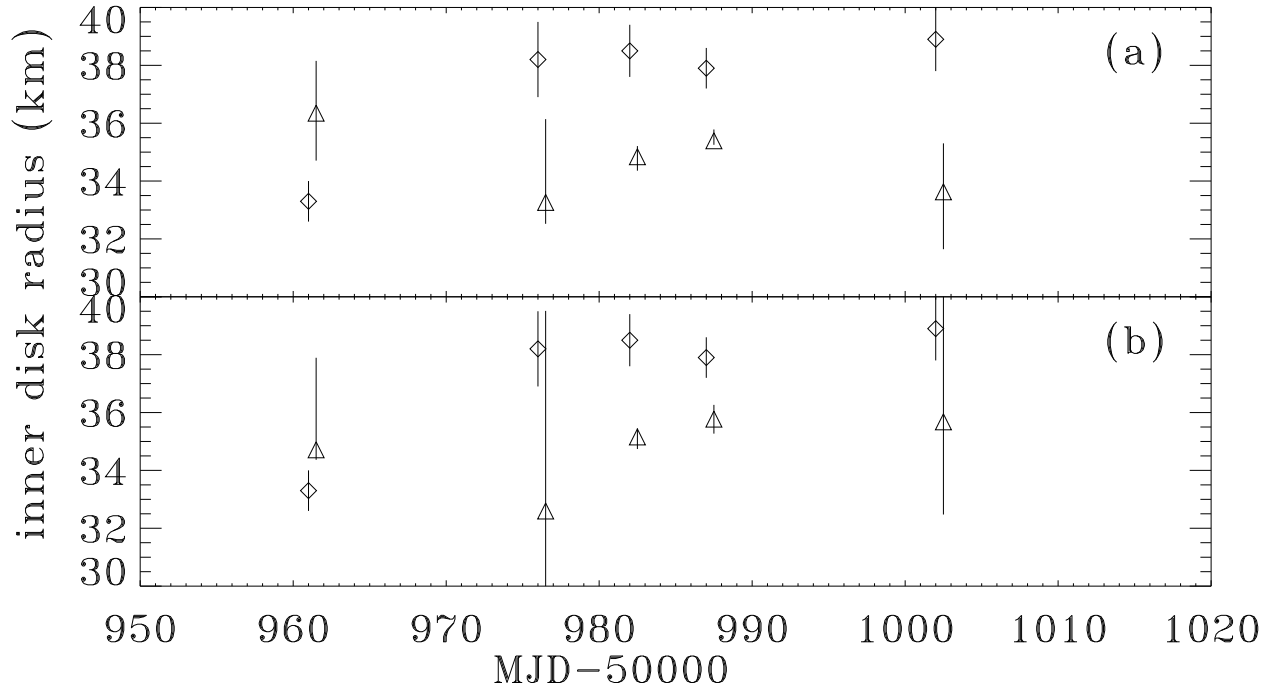


Fig. 5.— The inner radius of the accretion disk inferred from our table models (*triangle symbols*) for a spherical corona system (a) and for a disk-like corona system (b) and those derived from spectral-fitting with MCD+PL model (*diamond symbols*; Campana et al. 2002). In order to show the comparison clearly, we shift the observation date slightly in the plot.

Table 1: Results from spectral fits with our table models.

Date (MJD)	N_H (10^{22}cm^{-2})	T_{in} (keV)	T_c (keV)	R_c (R_g)	τ	θ ($^\circ$)	K_{norm}^a (km^2)	χ^2 (/dof)
Model A: spherical corona								
50961	$1.37_{+0.02}^{-0.01}$	$0.729_{+0.003}^{-0.001}$	200_{+**}^{-9}	20_{+4}^{-4}	$0.227_{+0.030}^{-0.028}$	25_{+21}^{-**}	1452_{+148}^{-128}	292(/242)
50976	$1.33_{+0.03}^{-0.03}$	$0.707_{+0.005}^{-0.004}$	200_{+**}^{-38}	10_{+16}^{-**}	$0.111_{+0.016}^{-0.111}$	23_{+40}^{-**}	1202_{+217}^{-53}	207(/170)
50982	$1.33_{+0.03}^{-0.02}$	$0.713_{+0.004}^{-0.003}$	100_{+10}^{-19}	49_{+18}^{-13}	$0.070_{+0.004}^{-0.006}$	59_{+5}^{-18}	2357_{+50}^{-65}	179(/195)
50987	$1.33_{+0.03}^{-0.01}$	$0.730_{+0.006}^{-0.002}$	$5.8_{+0.8}^{-**}$	99_{+10}^{-15}	$0.098_{+0.019}^{-0.004}$	$59(fix)$	2432_{+54}^{-19}	197(/148)
51002	$1.31_{+0.03}^{-0.01}$	$0.709_{+0.003}^{-0.003}$	$5.5_{+1.0}^{-0.5}$	99_{+20}^{-20}	$0.097_{+0.017}^{-0.017}$	29_{+46}^{-**}	1293_{+132}^{-148}	175(/149)
Model B: disk-like corona								
50961	$1.35_{+0.01}^{-0.02}$	$0.722_{+0.007}^{-0.003}$	200_{+**}^{-22}	–	$0.116_{+0.009}^{-0.007}$	18_{+16}^{-**}	1260_{+241}^{-25}	278(/243)
50976	$1.31_{+0.02}^{-0.03}$	$0.708_{+0.002}^{-0.003}$	200_{+**}^{-40}	–	$0.015_{+0.017}^{-0.003}$	69_{+4}^{-**}	2957_{+1388}^{-1231}	208(/171)
50982	$1.33_{+0.02}^{-0.02}$	$0.713_{+0.001}^{-0.002}$	100_{+9}^{-13}	–	$0.050_{+0.007}^{-0.005}$	18_{+28}^{-**}	1292_{+23}^{-30}	182(/196)
50987	$1.34_{+0.01}^{-0.01}$	$0.720_{+0.001}^{-0.002}$	$10.5_{+1.2}^{-0.5}$	–	$0.222_{+0.021}^{-0.013}$	53_{+16}^{-12}	2126_{+59}^{-59}	193(/149)
51002	$1.32_{+0.01}^{-0.02}$	$0.701_{+0.001}^{-0.004}$	$13.0_{+1.5}^{-0.7}$	–	$0.281_{+0.085}^{-0.061}$	37_{+26}^{-**}	1553_{+924}^{-266}	161(/150)

**the limit is not reachable.

^aNormalization of the table model, $K_{norm} = ((R_{in}/\text{km})/(D/10\text{kpc}))^2$.